

# Extracting the Energy-Dependent Neutrino-Nucleon Cross Section Above 10 TeV Using IceCube Showers

Mauricio Bustamante<sup>1,2,3,\*</sup> and Amy Connolly<sup>2,3,†</sup>

<sup>1</sup>*Niels Bohr International Academy & Discovery Center,  
Niels Bohr Institute, Blegdamsvej 17, 2100 Copenhagen, Denmark*

<sup>2</sup>*Center for Cosmology and AstroParticle Physics (CCAPP),  
The Ohio State University, Columbus, OH 43210, USA*

<sup>3</sup>*Department of Physics, The Ohio State University, Columbus, OH 43210, USA*

(Dated: January 12, 2019)

Neutrinos are key to probing the deep structure of matter and the high-energy Universe. Yet, until recently, their interactions had only been measured at laboratory energies up to about 350 GeV. An opportunity to measure their interactions at higher energies opened up with the detection of high-energy neutrinos in IceCube, partially of astrophysical origin. Scattering off matter inside the Earth affects the distribution of their arrival directions — from this, we extract the neutrino-nucleon cross section at energies from 18 TeV to 2 PeV, in four energy bins, in spite of uncertainties in the neutrino flux. Using six years of public IceCube High-Energy Starting Events, we explicitly show for the first time that the energy dependence of the cross section above 18 TeV agrees with the predicted softer-than-linear dependence, and reaffirm the absence of new physics that would make the cross section rise sharply, up to a center-of-mass energy  $\sqrt{s} \approx 1$  TeV.

**Introduction.**— Neutrino interactions, though feeble, are important for particle physics and astrophysics. They provide precise tests of the Standard Model [1–3], probes of new physics [4–6], and windows to otherwise veiled regions of the Universe. Yet, at neutrino energies above 350 GeV there had been no measurement of their interactions. This changed recently when the IceCube Collaboration found that the neutrino-nucleon cross section from 6.3 to 980 TeV agrees with predictions [7].

Because there is no artificial neutrino beam at a TeV and above, IceCube used atmospheric and astrophysical neutrinos, the latter discovered by them up to a few PeV [26, 31–38]. Refs. [4, 6, 39–42] showed that, because IceCube neutrinos interact significantly with matter inside Earth, their distribution in energy and arrival direction carries information about neutrino-nucleon cross sections, which, like IceCube [7], we extract.

However, Ref. [7] extracted the cross section in a single, wide energy bin, so its energy dependence in that range remains untested. A significant deviation from the predicted softer-than-linear dependence could signal the presence of new physics, so we extract the cross section in intervals from 18 TeV to 2 PeV. While Ref. [7] used only events born outside of IceCube we use instead only events born inside of it, which leads to a better handle on the neutrino energy.

Figure 1 shows that the cross section that we extract is compatible with the standard prediction. There is no indication of the sharp rise, at least below 1 PeV, predicted by some models of new physics [6, 43–51].

**Neutrino-nucleon cross section.**— Above a few GeV, neutrino-nucleon interactions are typically deep inelastic scatterings (DIS), where the neutrino scatters off

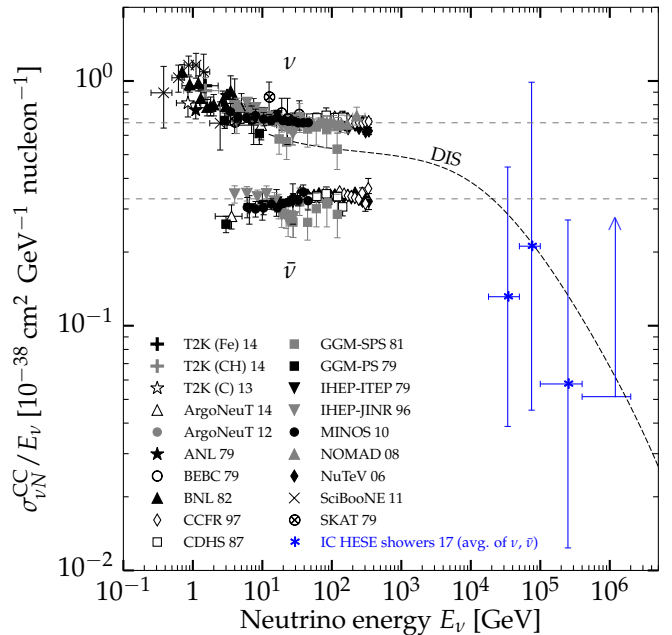


FIG. 1. Charged-current inclusive neutrino-nucleon cross section measurements [8–25]. The new results from this work, based on 6 years of IceCube HES showers [26–29], are an average between cross sections for  $\nu$  and  $\bar{\nu}$ , assuming equal astrophysical fluxes of each. In the highest-energy bin, we only set a lower limit ( $1\sigma$  shown). The thick dashed curve is a standard prediction of deep inelastic scattering (DIS), averaged between  $\nu$  and  $\bar{\nu}$ . Horizontal thin dashed lines are global averages from Ref. [30], which do not include the new results.

one of the constituent partons of the nucleon — a quark or a gluon. In both the charged-current (CC,  $\bar{\nu}_l + N \rightarrow l^{\mp} + X$ ) and neutral-current (NC,  $\bar{\nu}_l + N \rightarrow \bar{\nu}_l + X$ ) forms of this interaction, the nucleon  $N$  is broken up into par-

\* mbustamante@nbi.ku.dk; ORCID: 0000-0001-6923-0865

† connolly@physics.osu.edu; ORCID: 0000-0003-0049-5448

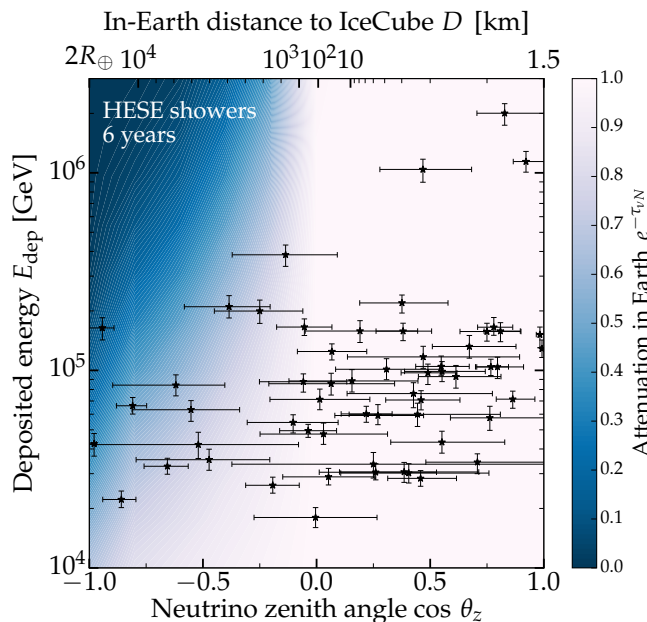


FIG. 2. Neutrino-induced showers from the IceCube 6-year HESE [26–29] sample. Neutrinos arrive from above ( $\cos \theta_z > 0$ ); from below, through the Earth ( $\cos \theta_z < 0$ ); and horizontally ( $\cos \theta_z = 0$ ). They travel a distance  $D$  inside the Earth (of radius  $R_\oplus = 6371$  km) to IceCube, buried at a depth of 1.5 km. The background shading represents the fraction of isotropic neutrino flux that survives after being attenuated by  $\nu N$  interactions inside the Earth, calculated using cross sections predicted in Ref. [59].

tons that hadronize into a final state  $X$ . The final-state hadrons carry a fraction  $y$  — the inelasticity — of the initial neutrino energy, while the final-state lepton carries the remaining fraction  $(1 - y)$ .

Calculation of the cross section  $\sigma_{\nu N}$  requires knowing the parton distribution functions (PDFs) in the nucleon. PDFs depend on two kinematic variables:  $Q^2 \equiv -q^2$ , the four-momentum transferred to the mediating  $W$  or  $Z$  boson, and the Bjorken scaling  $x$ , the fraction of nucleon momentum carried by the interacting parton [52]

To compute cross sections at neutrino energies  $E_\nu$  between TeV and PeV, we need PDFs evaluated at  $x \gtrsim m_W/E_\nu \sim 10^{-4}$ . Because these are known — at low  $x$ , from  $ep$  collisions in HERA [53, 54] — the uncertainty in the predicted TeV–PeV cross sections is small. Refs. [4, 55–65] have performed such calculations, some of which are shown in Fig. 3. Below  $\sim 10$  TeV, they yield  $\sigma_{\nu N} \propto E_\nu$ , revelatory of hard scattering off partons, and in agreement with data. Above  $\sim 10$  TeV, where  $Q^2 \sim m_W^2$ , they yield a softer-than-linear energy dependence, which has only been glimpsed in the available data up to 350 GeV [1–3].

**Detecting high-energy neutrinos.**— IceCube is the largest optical-Cherenkov neutrino detector. It consists of strings of photomultipliers buried deep in the clear Antarctic ice, instrumenting a volume of about  $1 \text{ km}^3$ .

Above TeV, CC interactions of  $\nu_e$  and  $\nu_\tau$  with nucleons in the ice, and NC interactions of all flavors, create localized particle showers, with roughly spherical Cherenkov-light profiles centered on the interaction vertex. CC interactions of  $\nu_\mu$  additionally create muons that make elongated tracks of Cherenkov light, several kilometers long and easily identifiable. (Other, flavor-specific signatures require energies higher than in our analysis [66–74].)

From the amount of collected light in a detected event, and its spatial and temporal profiles, IceCube infers its energy and arrival direction. But it cannot distinguish neutrinos from anti-neutrinos, or NC from CC showers, since they make similar light signals.

**Using contained showers only.**— Because cross sections vary with neutrino energy, we use exclusively a class of IceCube events where the incoming neutrino energy can be inferred using as few assumptions as possible. These are “starting events”, where the neutrino interaction was contained in the detector. Of these, we use only showers, not tracks, due not to a fundamental limitation, but to the IceCube data that is publicly available. Our approach differs from that of Ref. [7], which used only through-going muons, born in neutrino interactions outside the detector, for which estimation of the neutrino energy requires making important assumptions.

We use the publicly available 6-year sample of IceCube High Energy Starting Events (HESE) [26–29], consisting of 58 contained showers with deposited energies  $E_{\text{dep}}$  from 18 TeV to 2 PeV. Below a few tens of TeV, about half of the showers is due to atmospheric neutrinos and half to astrophysical neutrinos [29]; above, showers from astrophysical neutrinos dominate [75, 76].

Figure 2 shows the HESE showers distributed in  $E_{\text{dep}}$  and zenith angle  $\theta_z$ . Representative uncertainties are 10% in  $E_{\text{dep}}$  and  $15^\circ$  in  $\theta_z$  [77], which we adopt to describe the detector resolution. Showers are scarce above 200 TeV because the neutrino flux falls steeply with  $E_\nu$ .

In CC showers, the full neutrino energy is deposited in the ice, *i.e.*,  $E_{\text{dep}} \approx E_\nu$ , because both the outgoing electron or tau and the final-state hadrons shower. In NC showers, only a fraction  $y$  of the neutrino energy is deposited in the ice, *i.e.*,  $E_{\text{dep}} = yE_\nu$ , because only final-state hadrons shower. Standard calculations yield an average  $\langle y \rangle = 0.35$  at 10 TeV and 0.25 at 1 PeV [55]. Because of this low value and because the neutrino fluxes fall steeply with  $E_\nu$ , NC showers are nominally sub-dominant at any value of  $E_{\text{dep}}$ .

In starting tracks, the shower made by final-state hadrons is contained by the detector, but the muon track typically exits it. An assumption-free reconstruction of  $E_\nu$  requires knowing separately the energy of the hadronic shower  $E_{\text{sh}}$  and the muon energy loss rate  $dE_\mu/dX$ , which is proportional to the muon energy  $E_\mu$  [77]. Yet, while these quantities are known internally to the IceCube Collaboration, public data only provides, for each starting track, the total deposited energy,  $E_{\text{sh}} + |dE_\mu/dX|\Delta X$ , where  $\Delta X$  is the track length in the detector. Without additional information, in order

to deduce  $E_\nu$ , we would need to assume values of  $y$  and  $\Delta X$  for each event [78]. Hence, in keeping to our tenet of using few assumptions to deduce  $E_\nu$ , we do not include starting tracks in our analysis. This choice also reduces the chance of erroneously using a track created by an atmospheric muon, not a neutrino.

To use through-going muons in extracting the cross section, IceCube [7] inferred the most likely parent neutrino energy from the measured muon energy [77] by assuming the inelasticity distribution  $d\sigma_{\nu N}/dy$  from Ref. [59]. By using only contained showers, we forgo the need to assume an inelasticity distribution, and remain more sensitive to potential new physics that could modify it.

**Sensitivity to the cross section.**— Neutrino-nucleon interactions make the Earth opaque to neutrinos above 10 TeV, so neutrino fluxes are attenuated upon reaching IceCube. More neutrinos reach it from above — after crossing a few kilometers of ice — than from below — after crossing up to the diameter of the Earth.

A flux of incoming neutrinos with energy  $E_\nu$  and zenith angle  $\theta_z$  is attenuated by a factor  $e^{-\tau_{\nu N}(E_\nu, \theta_z)} \equiv \exp[-D(\theta_z)/L_{\nu N}(E_\nu, \theta_z)]$ , where  $\tau_{\nu N}$  is the opacity to  $\nu N$  interactions,  $D$  is the distance from the point of entry into Earth to IceCube, and  $L_{\nu N} = m_N / [(\sigma_{\nu N}^{\text{CC}}(E_\nu) + \sigma_{\nu N}^{\text{NC}}(E_\nu)) \langle \rho_\oplus(\theta_z) \rangle]$  is the neutrino interaction length. Here,  $\sigma_{\nu N}^{\text{CC}}$  and  $\sigma_{\nu N}^{\text{NC}}$  are, respectively, the CC and NC cross sections,  $m_N$  is the average nucleon mass in isoscalar matter, and  $\langle \rho_\oplus \rangle$  is the average matter density along this direction, calculated using the density profile from the Preliminary Reference Earth Model [55, 79]. Details are in the Supplemental Material, which includes Refs. [80–93]. Attenuation grows with the cross sections — which grow with  $E_\nu$  — and with  $D$ ; both effects are evident in the background shading in Fig. 2.

Within an energy interval, the number of events induced by a neutrino flux  $\Phi_\nu$  is  $N_{\text{sh}} \propto \Phi_\nu \cdot e^{-\tau_{\nu N}} \cdot \sigma_{\nu N}$ . Downgoing showers ( $\cos \theta_z > 0$ ) — unaffected by attenuation — fix the product  $\Phi_\nu \cdot \sigma_{\nu N}$ , while upgoing showers ( $\cos \theta_z < 0$ ) — affected by attenuation — break the degeneracy between  $\Phi_\nu$  and  $\sigma_{\nu N}$  via  $e^{-\tau_{\nu N}}$ , providing sensitivity to the cross sections.

**Extracting cross sections.**— We propagate atmospheric and astrophysical neutrinos through the Earth and produce test samples of contained showers in IceCube, taking into account its energy and angular resolution; see the Supplemental Material. To extract the cross sections, we compare the distributions in  $E_{\text{dep}}$  and  $\cos \theta_z$  of the test showers — generated with varying values of the cross sections — to the distribution observed by IceCube.

To probe the energy dependence of the cross sections, we bin showers in  $E_{\text{dep}}$  and extract the cross section from data in each bin independently of the others. Except for global assumptions on detector resolution and the choice of atmospheric neutrino spectrum (see below), parameters extracted in different bins are uncorrelated.

The first three bins contain comparable numbers of showers: 18–50 TeV (17 showers), 50–100 TeV (18 show-

ers), and 100–400 TeV (20 showers). The final bin, 400–2004 TeV, contains only 3 downgoing showers, between 1–2 PeV. Due to their short travel distances ( $D \lesssim 10$  km) and negligible expected attenuation, in this bin we only set a lower limit on the cross section. This stresses the need for upgoing HESE events above 400 TeV.

For atmospheric neutrinos, we use the most recent calculation of the  $\nu_e$ ,  $\bar{\nu}_e$ ,  $\nu_\mu$ , and  $\bar{\nu}_\mu$  fluxes from pion and kaon decays from Ref. [94]. Their zenith-angle distribution at the South Pole, though anisotropic, is symmetric around  $\cos \theta_z = 0$ , so it does not introduce spurious directional asymmetries. We do not include a contribution from prompt atmospheric neutrinos [95–108], since searches have failed to find evidence of them [26, 31–38]. We include the self-veto [109, 110] used by the HESE analysis to reduce the atmospheric contribution.

For astrophysical neutrinos, we assume, independently in each energy bin, an isotropic power-law energy spectrum  $\Phi_\nu \propto E_\nu^{-\gamma}$  for all flavors of neutrinos and anti-neutrinos, in agreement with theoretical expectations [111] and IceCube findings [112]. The value of  $\gamma$  is obtained from a fit to data in each bin. This makes our results robust against variations with energy of the spectral shape of astrophysical neutrinos, unlike Ref. [7], which assumed a single power law spanning the range 6.3–980 TeV. We assume flavor equipartition, as expected from standard mixing [68, 78, 113–117] and in agreement with data [36, 118]. Because IceCube cannot distinguish neutrinos from anti-neutrinos, we can only extract a combination of their cross sections, each weighed by its corresponding flux. We assume the likely case [119, 120] of equal fluxes, coming, *e.g.*, from proton-proton interactions [121].

**Assumptions.**— Because data is scant, to reduce the number of free parameters to fit, we make three reasonable assumptions inspired on standard high-energy predictions. With more data, they could be tested.

First, the rate of CC showers dominates over the rate of NC showers at any value of  $E_{\text{dep}}$ , based on the arguments above. For simplicity, we adopt a constant  $\langle y \rangle = 0.25$  for NC showers. This assumption allows us to express the extracted cross section as a function of  $E_\nu \approx E_{\text{dep}}$ .

Second, CC cross sections dominate over NC cross sections. We assume  $\sigma_{\nu N}^{\text{NC}} = \sigma_{\nu N}^{\text{CC}}/3$  and  $\sigma_{\bar{\nu} N}^{\text{NC}} = \sigma_{\bar{\nu} N}^{\text{CC}}/3$ , following, *e.g.*, Ref. [4]. This assumption allows us to fit only for CC cross sections.

Third, the ratio of  $\bar{\nu} N$  to  $\nu N$  cross sections is fixed in each bin. Hence, when fitting,  $\sigma_{\bar{\nu} N}^{\text{CC}} = \langle \sigma_{\bar{\nu} N}^{\text{CC}} / \sigma_{\nu N}^{\text{CC}} \rangle \cdot \sigma_{\nu N}^{\text{CC}}$ , where  $\langle \sigma_{\bar{\nu} N}^{\text{CC}} / \sigma_{\nu N}^{\text{CC}} \rangle$  is the average ratio in that bin predicted by Ref. [59] (see Table I). This assumption allows us to fit only for  $\nu N$  cross sections.

Thus, within each energy bin, we independently vary only the  $\nu N$  CC cross section  $\sigma_{\nu N}^{\text{CC}}$  and three nuisance parameters — the number of showers due to atmospheric neutrinos  $N_{\text{sh}}^{\text{atm}}$ , the number of showers due to astrophysical neutrinos  $N_{\text{sh}}^{\text{ast}}$ , and the astrophysical spectral index  $\gamma$ . To avoid introducing bias, we assume flat priors for all of them. For each choice of values, we compare our

TABLE I. Neutrino-nucleon charged-current inclusive cross sections, averaged between neutrinos ( $\sigma_{\nu N}^{\text{CC}}$ ) and anti-neutrinos ( $\sigma_{\bar{\nu} N}^{\text{CC}}$ ), extracted from 6 years of IceCube HESE showers. To obtain these results, we fixed  $\sigma_{\nu N}^{\text{CC}} = \langle \sigma_{\bar{\nu} N}^{\text{CC}} / \sigma_{\nu N}^{\text{CC}} \rangle \cdot \sigma_{\nu N}^{\text{CC}}$  — where  $\langle \sigma_{\bar{\nu} N}^{\text{CC}} / \sigma_{\nu N}^{\text{CC}} \rangle$  is the average ratio of  $\bar{\nu}$  to  $\nu$  cross sections calculated using the standard prediction from Ref. [59] — and  $\sigma_{\nu N}^{\text{NC}} = \sigma_{\nu N}^{\text{CC}}/3$ ,  $\sigma_{\bar{\nu} N}^{\text{NC}} = \sigma_{\bar{\nu} N}^{\text{CC}}/3$ . Uncertainties are  $1\sigma$ , statistical plus systematic, added in quadrature.

$E_\nu$ [TeV]	$\langle E_\nu \rangle$ [TeV]	$\langle \sigma_{\bar{\nu} N}^{\text{CC}} / \sigma_{\nu N}^{\text{CC}} \rangle$	$\log_{10}[\frac{1}{2}(\sigma_{\nu N}^{\text{CC}} + \sigma_{\bar{\nu} N}^{\text{CC}})/\text{cm}^2]$
18–50	32	0.752	$-34.35 \pm 0.53$
50–100	75	0.825	$-33.80 \pm 0.67$
100–400	250	0.888	$-33.84 \pm 0.67$
400–2004	1202	0.957	$> -33.21 (1\sigma)$

test shower spectrum to the HESE shower spectrum via a likelihood. To find the best-fit values of the parameters, we maximize the likelihood. The Supplemental Material describes the statistical analysis in detail.

**Results.**— Table I shows the extracted cross section, marginalized over the nuisance parameters. Because  $\sigma_{\nu N}$  and  $\sigma_{\bar{\nu} N}$  are not independent in the fit, we present their average there and in Figs. 2 and 3.

Figure 3 shows that, in each bin, results agree within  $1\sigma$  with widely used standard predictions. The IceCube Collaboration has adopted the cross section from Cooper-Sarkar *et al.* [59]. We include other calculations for comparison [4, 55, 56, 60, 62]. All predictions are consistent with our measurements within errors.

Our results are consistent with the IceCube analysis [7], which found a cross section compatible with Ref. [59]. Their smaller uncertainty is due to using  $\sim 10^4$  through-going muons. However, by grouping all events in a single energy bin, their analysis did not probe the energy dependence of the cross section. Like that analysis, our results are also consistent with standard cross-section predictions, but in narrower energy intervals.

Because the number of showers in each bin is small, statistical fluctuations weaken the interplay of downgoing versus upgoing showers described above. To isolate the dominant statistical uncertainty, we minimized again the likelihood, this time keeping the nuisance parameters fixed at their best-fit values (see Table II in the Supplemental Material). The resulting uncertainty, attributed to statistics only, is 0.51, 0.63, and 0.62 in the first three bins, where we have a measurement. The systematic uncertainty, obtained by subtracting these values in quadrature from the total uncertainties in Table I is 0.14, 0.23, and 0.25 in each bin, slightly higher than in Ref. [7], due to a less detailed modeling of the detector. While Ref. [7] found comparable statistical and systematic uncertainties, we are presently dominated by statistics, since it uses an event sample that is smaller by a factor of  $\sim 200$ .

Nevertheless, our results disfavor new-physics models where the cross section rises sharply below 1 PeV [6, 44–51]. Figure 3 shows as example a model of TeV-

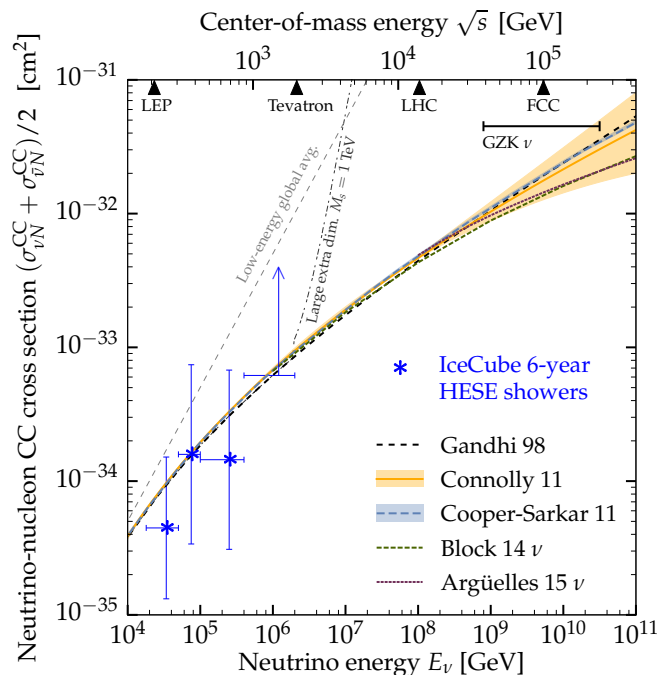


FIG. 3. Neutrino-nucleon charged-current cross section, averaged for neutrinos and anti-neutrinos, from different predictions (lines) [4, 56, 59, 60, 62], compared to measurements from this work (stars). The low-energy global average [30] has the linear dependence on  $E_\nu$  appropriate below  $\sim 10$  TeV. The model of large extra dimensions, included for illustration, is from Ref. [43] (quantum-gravity scale of 1 TeV and all partial waves summed), corrected here to match modern standard predictions of the cross section below 1 PeV.

scale gravity with large extra dimensions [43]. While this model was disfavored by the LHC [122, 123], we provide independent confirmation via a different channel. More stringent tests of new-physics models, beyond the scope of this letter, should also consider the effect of modifications to the inelasticity distribution.

**Limitations and improvements.**— IceCube is sparsely instrumented and designed to detect the enormous light imprints made by high-energy neutrinos. Except for high-energy muons, it cannot track individual particles or reconstruct  $Q^2$  and  $x$ , unlike densely instrumented detectors. Hence, we can only extract the cross section as a function of energy, integrated over other kinematic variables. While we cannot extract individual PDFs, we can test their combination in the cross section.

Further, IceCube cannot distinguish if a particular shower was made in a CC or an NC interaction, and by a neutrino or an anti-neutrino. The differences are too subtle to unequivocally identify them in individual showers [124], but it might be possible to extract them statistically from a large enough data sample [125].

Lastly, we assumed that the astrophysical neutrino flux is isotropic [36, 126, 127]. Nevertheless, there are hints of a Galactic contribution [36, 126, 128, 129], with data

allowing  $< 14\%$  of the all-sky flux to come from the Galactic Plane [127]. If a Galactic flux is discovered, future cross-section analyses will need to acknowledge its anisotropy to avoid incorrectly attributing the distribution of arrival directions solely to in-Earth attenuation.

**Summary and outlook.**— We have extracted the energy dependence of the neutrino-nucleon cross section at energies beyond those available in man-made neutrino beams, making use of the high-energy reach of IceCube. Our results are compatible with predictions based on nucleon structure extracted from scattering experiments at lower energies and disfavor extreme deviations that could stem from new physics in the TeV–PeV range.

It would be straightforward to repeat the present analysis using a larger HESE shower sample. The proposed upgrade IceCube-Gen2 [130] could have an event rate 5–7 times higher, thus reducing the impact of random fluctuations. These showers could be combined with showers from the upcoming KM3NeT detector [131]; their improved angular resolution of  $\sim 2^\circ$  above 50 TeV would allow for better estimates of in-Earth attenuation. Starting tracks can also be considered, as long as one does not rely on predictions of the inelasticity distribution to reconstruct the parent neutrino energy.

An interesting possibility is to measure the inelasticity distribution [132]. This can be done using starting tracks where the hadronic shower energy  $E_{\text{sh}}$  and the outgoing muon energy  $E_\mu$  are known individually, in order to reconstruct the inelasticity  $y = (1 + E_\mu/E_{\text{sh}})^{-1}$  [133, 134].

At the EeV scale, differences between cross-section predictions increase. Measuring  $\sigma_{\nu N}$  at these energies would probe  $x \sim m_W/E_\nu \lesssim 10^{-6}$ , beyond the reach of laboratory scattering experiments. This would prove instrumental in testing not only new physics, but also predictions of the potentially non-linear behavior of PDFs at low  $x$ , such as from BFKL theory [135–138] and color-glass condensates [139]; see, *e.g.*, Ref. [63, 140, 141]. However, because the predicted neutrino flux at these energies, while uncertain, is smaller than at PeV, precision measurements of the cross section will likely be limited by statistics; see Ref. [142] for details. Nevertheless, large-volume neutrino detectors like ARA [143–145], AR-IANNA [146, 147], GRAND [148], and POEMMA [149], might differentiate [150] between predictions, provided the event rate is high enough.

## ACKNOWLEDGEMENTS

MB is supported in part by NSF Grants PHY-1404311 and PHY-1714479, and by the Danmarks Grundforskningsfond Grant 1041811001. AC is supported by NSF CAREER award 1255557. This work used resources provided by the Ohio Supercomputer Center. We thank Patrick Allison, John Beacom, Francis Halzen, Spencer Klein, Shirley Li, and Subir Sarkar for useful feedback and discussion.

- 
- [1] Raymond Brock *et al.* (CTEQ), “Handbook of perturbative QCD: Version 1.0,” *Rev. Mod. Phys.* **67**, 157–248 (1995).
  - [2] Janet M. Conrad, Michael H. Shaevitz, and Tim Bolton, “Precision measurements with high-energy neutrino beams,” *Rev. Mod. Phys.* **70**, 1341–1392 (1998), arXiv:hep-ex/9707015 [hep-ex].
  - [3] J. A. Formaggio and G. P. Zeller, “From eV to EeV: Neutrino Cross Sections Across Energy Scales,” *Rev. Mod. Phys.* **84**, 1307–1341 (2012), arXiv:1305.7513 [hep-ex].
  - [4] Amy Connolly, Robert S. Thorne, and David Waters, “Calculation of High Energy Neutrino-Nucleon Cross Sections and Uncertainties Using the MSTW Parton Distribution Functions and Implications for Future Experiments,” *Phys. Rev. D* **83**, 113009 (2011), arXiv:1102.0691 [hep-ph].
  - [5] Chien-Yi Chen, P. S. Bhupal Dev, and Amarjit Soni, “Standard model explanation of the ultrahigh energy neutrino events at IceCube,” *Phys. Rev. D* **89**, 033012 (2014), arXiv:1309.1764 [hep-ph].
  - [6] D. Marfatia, D. W. McKay, and T. J. Weiler, “New physics with ultra-high-energy neutrinos,” *Phys. Lett. B* **748**, 113–116 (2015), arXiv:1502.06337 [hep-ph].
  - [7] M. G. Aartsen *et al.* (IceCube), “Measurement of the multi-TeV neutrino cross section with IceCube using Earth absorption,” *Nature* (2017), 10.1038/nature24459, arXiv:1711.08119 [hep-ex].
  - [8] A. I. Mukhin *et al.*, “Energy Dependence of Total Cross-sections for Neutrino and Anti-neutrino Interactions at Energies Below 35-GeV,” *Sov. J. Nucl. Phys.* **30**, 528 (1979), [*Yad. Fiz.* 30, 1014 (1979)].
  - [9] D. S. Baranov *et al.*, “Measurements of the  $\nu_\mu N$  Total Cross-section at 2-GeV - 30-GeV in Skat Neutrino Experiment,” *Phys. Lett. B* **81**, 255–257 (1979).
  - [10] S. J. Barish *et al.*, “Study of Neutrino Interactions in Hydrogen and Deuterium: Inelastic Charged Current Reactions,” *Phys. Rev. D* **19**, 2521 (1979).
  - [11] S. Ciampolillo *et al.* (Aachen-Brussels-CERN-Ecole Poly-Orsay-Padua, Gargamelle Neutrino Propane), “Total Cross-section for Neutrino Charged Current Interactions at 3-GeV and 9-GeV,” *Phys. Lett. B* **84**, 281–284 (1979).
  - [12] J. G. H. de Groot *et al.*, “Inclusive Interactions of High-Energy Neutrinos and anti-neutrinos in Iron,” *Z. Phys. C* **1**, 143 (1979).
  - [13] D. C. Colley *et al.*, “Cross-sections for Charged Current Neutrino and Anti-neutrino Interactions in the Energy Range 10-GeV to 50-GeV,” *Z. Phys. C* **2**, 187 (1979).
  - [14] J. G. Morfin *et al.* (Gargamelle SPS), “Total Cross-sections and Nucleon Structure Functions in the Gargamelle SPS Neutrino / Anti-neutrino Experiment,” *Phys. Lett. B* **104**, 235–238 (1981).
  - [15] N. J. Baker *et al.*, “Total Cross-sections for Muon-neutrino  $N$  and Muon-neutrino  $P$  Charged Current Interactions in the 7-ft Bubble Chamber,” *Phys. Rev. D*



- 25, 617–623 (1982).
- [16] J. P. Berge *et al.*, “Total Neutrino and Anti-neutrino Charged Current Cross-section Measurements in 100-GeV, 160-GeV and 200-GeV Narrow Band Beams,” *Z. Phys. C* **35**, 443 (1987).
- [17] V. B. Anikeev *et al.*, “Total cross-section measurements for muon-neutrino, anti-muon-neutrino interactions in 3-GeV–30-GeV energy range with IHEP-JINR neutrino detector,” *Z. Phys. C* **70**, 39–46 (1996).
- [18] W. G. Seligman, *A Next-to-Leading Order QCD Analysis of Neutrino-Iron Structure Functions at the Tevatron*, Ph.D. thesis, Columbia University (1997).
- [19] M. Tzanov *et al.* (NuTeV), “Precise measurement of neutrino and anti-neutrino differential cross sections,” *Phys. Rev. D* **74**, 012008 (2006), arXiv:hep-ex/0509010 [hep-ex].
- [20] Q. Wu *et al.* (NOMAD), “A Precise measurement of the muon neutrino-nucleon inclusive charged current cross-section off an isoscalar target in the energy range  $2.5 < E_\nu < 40$  GeV by NOMAD,” *Phys. Lett. B* **660**, 19–25 (2008), arXiv:0711.1183 [hep-ex].
- [21] P. Adamson *et al.* (MINOS), “Neutrino and Antineutrino Inclusive Charged-current Cross Section Measurements with the MINOS Near Detector,” *Phys. Rev. D* **81**, 072002 (2010), arXiv:0910.2201 [hep-ex].
- [22] Y. Nakajima *et al.* (SciBooNE), “Measurement of inclusive charged current interactions on carbon in a few-GeV neutrino beam,” *Phys. Rev. D* **83**, 012005 (2011), arXiv:1011.2131 [hep-ex].
- [23] K. Abe *et al.* (T2K), “Measurement of the inclusive  $\nu_\mu$  charged current cross section on carbon in the near detector of the T2K experiment,” *Phys. Rev. D* **87**, 092003 (2013), arXiv:1302.4908 [hep-ex].
- [24] R. Acciarri *et al.* (ArgoNeuT), “Measurements of Inclusive Muon Neutrino and Antineutrino Charged Current Differential Cross Sections on Argon in the NuMI Antineutrino Beam,” *Phys. Rev. D* **89**, 112003 (2014), arXiv:1404.4809 [hep-ex].
- [25] K. Abe *et al.* (T2K), “Measurement of the inclusive  $\nu_\mu$  charged current cross section on iron and hydrocarbon in the T2K on-axis neutrino beam,” *Phys. Rev. D* **90**, 052010 (2014), arXiv:1407.4256 [hep-ex].
- [26] M. G. Aartsen *et al.* (IceCube), “Observation of High-Energy Astrophysical Neutrinos in Three Years of IceCube Data,” *Phys. Rev. Lett.* **113**, 101101 (2014), arXiv:1405.5303 [astro-ph.HE].
- [27] Claudio Kopper, William Giang, and Naoko Kurahashi (IceCube), “Observation of Astrophysical Neutrinos in Four Years of IceCube Data,” *Proceedings, 34th International Cosmic Ray Conference (ICRC 2015): The Hague, The Netherlands, July 30-August 6, 2015*, PoS **ICRC2015**, 1081 (2016).
- [28] IceCube Collaboration, *Observation of Astrophysical Neutrinos in Four Years of IceCube Data* (2015 (accessed October 21, 2015)).
- [29] Claudio Kopper, “Observation of Astrophysical Neutrinos in Six Years of IceCube Data,” Talk given at the International Cosmic Ray Conference 2017, July 15, 2017, Busan, <https://indico.snu.ac.kr/indico/event/>.
- [30] C. Patrignani *et al.* (Particle Data Group), “Review of Particle Physics,” *Chin. Phys. C* **40**, 100001 (2016).
- [31] M. G. Aartsen *et al.* (IceCube), “First observation of PeV-energy neutrinos with IceCube,” *Phys. Rev. Lett.* **111**, 021103 (2013), arXiv:1304.5356 [astro-ph.HE].
- [32] M. G. Aartsen *et al.* (IceCube), “Evidence for High-Energy Extraterrestrial Neutrinos at the IceCube Detector,” *Science* **342**, 1242856 (2013), arXiv:1311.5238 [astro-ph.HE].
- [33] M. G. Aartsen *et al.* (IceCube), “Search for a diffuse flux of astrophysical muon neutrinos with the IceCube 59-string configuration,” *Phys. Rev. D* **89**, 062007 (2014), arXiv:1311.7048 [astro-ph.HE].
- [34] M. G. Aartsen *et al.* (IceCube), “Atmospheric and astrophysical neutrinos above 1 TeV interacting in IceCube,” *Phys. Rev. D* **91**, 022001 (2015), arXiv:1410.1749 [astro-ph.HE].
- [35] M. G. Aartsen *et al.* (IceCube), “Measurement of the Atmospheric  $\nu_e$  Spectrum with IceCube,” *Phys. Rev. D* **91**, 122004 (2015), arXiv:1504.03753 [astro-ph.HE].
- [36] M. G. Aartsen *et al.* (IceCube), “A combined maximum-likelihood analysis of the high-energy astrophysical neutrino flux measured with IceCube,” *Astrophys. J.* **809**, 98 (2015), arXiv:1507.03991 [astro-ph.HE].
- [37] M. G. Aartsen *et al.* (IceCube), “Evidence for Astrophysical Muon Neutrinos from the Northern Sky with IceCube,” *Phys. Rev. Lett.* **115**, 081102 (2015), arXiv:1507.04005 [astro-ph.HE].
- [38] M. G. Aartsen *et al.* (IceCube), “Observation and Characterization of a Cosmic Muon Neutrino Flux from the Northern Hemisphere using six years of IceCube data,” *Astrophys. J.* **833**, 3 (2016), arXiv:1607.08006 [astro-ph.HE].
- [39] Dan Hooper, “Measuring high-energy neutrino nucleon cross-sections with future neutrino telescopes,” *Phys. Rev. D* **65**, 097303 (2002), arXiv:hep-ph/0203239 [hep-ph].
- [40] S. Hussain, D. Marfatia, D. W. McKay, and D. Seckel, “Cross section dependence of event rates at neutrino telescopes,” *Phys. Rev. Lett.* **97**, 161101 (2006), arXiv:hep-ph/0606246 [hep-ph].
- [41] E. Borriello, A. Cuoco, G. Mangano, G. Miele, S. Pastor, O. Pisanti, and P. D. Serpico, “Disentangling neutrino-nucleon cross section and high energy neutrino flux with a  $\text{km}^3$  neutrino telescope,” *Phys. Rev. D* **77**, 045019 (2008), arXiv:0711.0152 [astro-ph].
- [42] S. Hussain, D. Marfatia, and D. W. McKay, “Upward shower rates at neutrino telescopes directly determine the neutrino flux,” *Phys. Rev. D* **77**, 107304 (2008), arXiv:0711.4374 [hep-ph].
- [43] J. Alvarez-Muniz, F. Halzen, Tao Han, and D. Hooper, “Phenomenology of high-energy neutrinos in low scale quantum gravity models,” *Phys. Rev. Lett.* **88**, 021301 (2002), arXiv:hep-ph/0107057 [hep-ph].
- [44] Jaime Alvarez-Muniz, Jonathan L. Feng, Francis Halzen, Tao Han, and Dan Hooper, “Detecting microscopic black holes with neutrino telescopes,” *Phys. Rev. D* **65**, 124015 (2002), arXiv:hep-ph/0202081 [hep-ph].
- [45] Luis A. Anchordoqui, Jonathan L. Feng, Haim Goldberg, and Alfred D. Shapere, “Updated limits on TeV scale gravity from absence of neutrino cosmic ray showers mediated by black holes,” *Phys. Rev. D* **68**, 104025 (2003), arXiv:hep-ph/0307228 [hep-ph].
- [46] Eun-Joo Ahn, Marco Cavaglia, and Angela V Olinto, “Uncertainties in limits on TeV gravity from neutrino induced air showers,” *Astropart. Phys.* **22**, 377–385 (2005), arXiv:hep-ph/0312249 [hep-ph].
- [47] J. I. Illana, M. Masip, and D. Meloni, “Cosmogenic neutrinos and signals of TeV gravity in air showers and neu-

- trino telescopes,” *Phys. Rev. Lett.* **93**, 151102 (2004), arXiv:hep-ph/0402279 [hep-ph].
- [48] Shahid Hussain and Douglas W. McKay, “Bounds on low scale gravity from RICE data and cosmogenic neutrino flux models,” *Phys. Lett. B* **634**, 130–136 (2006), arXiv:hep-ph/0510083 [hep-ph].
- [49] Luis A. Anchordoqui, Matthew M. Glenz, and Leonard Parker, “Black Holes at IceCube Neutrino Telescope,” *Phys. Rev. D* **75**, 024011 (2007), arXiv:hep-ph/0610359 [hep-ph].
- [50] Joseph Lykken, Olga Mena, and Soebur Razzaque, “Ultrahigh-energy neutrino flux as a probe of large extra-dimensions,” *JCAP* **0712**, 015 (2007), arXiv:0705.2029 [hep-ph].
- [51] Luis A. Anchordoqui *et al.*, “Using cosmic neutrinos to search for non-perturbative physics at the Pierre Auger Observatory,” *Phys. Rev. D* **82**, 043001 (2010), arXiv:1004.3190 [hep-ph].
- [52] Carlo Giunti and Chung W. Kim, *Fundamentals of Neutrino Physics and Astrophysics* (2007).
- [53] F. D. Aaron *et al.* (ZEUS, H1), “Combined Measurement and QCD Analysis of the Inclusive  $e^+p$  Scattering Cross Sections at HERA,” *JHEP* **01**, 109 (2010), arXiv:0911.0884 [hep-ex].
- [54] H. Abramowicz *et al.* (ZEUS, H1), “Combination of measurements of inclusive deep inelastic  $e^\pm p$  scattering cross sections and QCD analysis of HERA data,” *Eur. Phys. J. C* **75**, 580 (2015), arXiv:1506.06042 [hep-ex].
- [55] Raj Gandhi, Chris Quigg, Mary Hall Reno, and Ina Sarcevic, “Ultrahigh-energy neutrino interactions,” *Astropart. Phys.* **5**, 81–110 (1996), arXiv:hep-ph/9512364.
- [56] Raj Gandhi, Chris Quigg, Mary Hall Reno, and Ina Sarcevic, “Neutrino interactions at ultrahigh energies,” *Phys. Rev. D* **58**, 093009 (1998), hep-ph/9807264.
- [57] Amanda Cooper-Sarkar and Subir Sarkar, “Predictions for high energy neutrino cross-sections from the ZEUS global PDF fits,” *JHEP* **01**, 075 (2008), arXiv:0710.5303 [hep-ph].
- [58] M. Gluck, P. Jimenez-Delgado, and E. Reya, “On the charged current neutrino-nucleon total cross section at high energies,” *Phys. Rev. D* **81**, 097501 (2010), arXiv:1003.3168 [hep-ph].
- [59] Amanda Cooper-Sarkar, Philipp Mertsch, and Subir Sarkar, “The high energy neutrino cross-section in the Standard Model and its uncertainty,” *JHEP* **08**, 042 (2011), arXiv:1106.3723 [hep-ph].
- [60] Martin M. Block, Loyal Durand, and Phuoc Ha, “Connection of the virtual  $\gamma^*p$  cross section of ep deep inelastic scattering to real  $\gamma p$  scattering, and the implications for  $\nu N$  and  $ep$  total cross sections,” *Phys. Rev. D* **89**, 094027 (2014), arXiv:1404.4530 [hep-ph].
- [61] V. P. Goncalves and D. R. Gratieri, “Estimating nonlinear QCD effects in ultrahigh energy neutrino events at IceCube,” *Phys. Rev. D* **90**, 057502 (2014), arXiv:1406.5890 [hep-ph].
- [62] Carlos A. Argüelles, Francis Halzen, Logan Wille, Mike Kroll, and Mary Hall Reno, “High-energy behavior of photon, neutrino, and proton cross sections,” *Phys. Rev. D* **92**, 074040 (2015), arXiv:1504.06639 [hep-ph].
- [63] Javier L. Albacete, Jose I. Illana, and Alba Soto-Ontoso, “Neutrino-nucleon cross section at ultrahigh energy and its astrophysical implications,” *Phys. Rev. D* **92**, 014027 (2015), arXiv:1505.06583 [hep-ph].
- [64] Rhorry Gauld and Juan Rojo, “Precision determination of the small- $x$  gluon from charm production at LHCb,” *Phys. Rev. Lett.* **118**, 072001 (2017), arXiv:1610.09373 [hep-ph].
- [65] Richard D. Ball, Valerio Bertone, Marco Bonvini, Simone Marzani, Juan Rojo, and Luca Rottoli, “Parton distributions with small- $x$  resummation: evidence for BFKL dynamics in HERA data,” (2017), arXiv:1710.05935 [hep-ph].
- [66] Sheldon L. Glashow, “Resonant Scattering of Antineutrinos,” *Phys. Rev.* **118**, 316–317 (1960).
- [67] John G. Learned and Sandip Pakvasa, “Detecting tau-neutrino oscillations at PeV energies,” *Astropart. Phys.* **3**, 267–274 (1995), arXiv:hep-ph/9405296.
- [68] John F. Beacom, Nicole F. Bell, Dan Hooper, Sandip Pakvasa, and Thomas J. Weiler, “Measuring flavor ratios of high-energy astrophysical neutrinos,” *Phys. Rev. D* **68**, 093005 (2003), [Erratum: *Phys. Rev. D* **72**, 019901 (2005)], arXiv:hep-ph/0307025.
- [69] Edgar Bugaev, Teresa Montaruli, Yuri Shlepin, and Igor A. Sokalski, “Propagation of tau neutrinos and tau leptons through the earth and their detection in underwater / ice neutrino telescopes,” *Astropart. Phys.* **21**, 491–509 (2004), arXiv:hep-ph/0312295 [hep-ph].
- [70] Luis A. Anchordoqui, Haim Goldberg, Francis Halzen, and Thomas J. Weiler, “Neutrinos as a diagnostic of high energy astrophysical processes,” *Phys. Lett. B* **B621**, 18–21 (2005), arXiv:hep-ph/0410003.
- [71] Atri Bhattacharya, Raj Gandhi, Werner Rodejohann, and Atsushi Watanabe, “The Glashow resonance at IceCube: signatures, event rates and  $pp$  vs.  $p\gamma$  interactions,” *JCAP* **1110**, 017 (2011), arXiv:1108.3163 [astro-ph.HE].
- [72] Atri Bhattacharya, Raj Gandhi, Werner Rodejohann, and Atsushi Watanabe, “On the interpretation of IceCube cascade events in terms of the Glashow resonance,” (2012), arXiv:1209.2422 [hep-ph].
- [73] V. Barger, Lingjun Fu, J. G. Learned, D. Marfatia, S. Pakvasa, and T. J. Weiler, “Glashow resonance as a window into cosmic neutrino sources,” *Phys. Rev. D* **90**, 121301 (2014), arXiv:1407.3255 [astro-ph.HE].
- [74] Andrea Palladino, Giulia Pagliaroli, Francesco L. Villante, and Francesco Vissani, “Double pulses and cascades above 2 PeV in IceCube,” *Eur. Phys. J. C* **76**, 52 (2016), arXiv:1510.05921 [astro-ph.HE].
- [75] John F. Beacom and Julian Candia, “Shower power: Isolating the prompt atmospheric neutrino flux using electron neutrinos,” *JCAP* **0411**, 009 (2004), arXiv:hep-ph/0409046 [hep-ph].
- [76] Ranjan Laha, John F. Beacom, Basudeb Dasgupta, Shunsaku Horiuchi, and Kohta Murase, “Demystifying the PeV Cascades in IceCube: Less (Energy) is More (Events),” *Phys. Rev. D* **88**, 043009 (2013), arXiv:1306.2309 [astro-ph.HE].
- [77] M. G. Aartsen *et al.* (IceCube), “Energy Reconstruction Methods in the IceCube Neutrino Telescope,” *JINST* **9**, P03009 (2014), arXiv:1311.4767 [physics.ins-det].
- [78] Sergio Palomares-Ruiz, Aaron C. Vincent, and Olga Mena, “Spectral analysis of the high-energy IceCube neutrinos,” *Phys. Rev. D* **91**, 103008 (2015), arXiv:1502.02649 [astro-ph.HE].
- [79] A. M. Dziewonski and D. L. Anderson, “Preliminary Reference Earth Model,” *Phys. Earth Planet. Interiors* **25**, 297–356 (1981).

- [80] Farhan Feroz and M. P. Hobson, “Multimodal nested sampling: an efficient and robust alternative to MCMC methods for astronomical data analysis,” *Mon. Not. Roy. Astron. Soc.* **384**, 449 (2008), arXiv:0704.3704 [astro-ph].
- [81] S. R. Kelner and F. A. Aharonian, “Energy spectra of gamma-rays, electrons and neutrinos produced at interactions of relativistic protons with low energy radiation,” *Phys. Rev. D* **78**, 034013 (2008), arXiv:0803.0688 [astro-ph].
- [82] F. Feroz, M. P. Hobson, and M. Bridges, “MultiNest: an efficient and robust Bayesian inference tool for cosmology and particle physics,” *Mon. Not. Roy. Astron. Soc.* **398**, 1601–1614 (2009), arXiv:0809.3437 [astro-ph].
- [83] S. Hümmer, M. Rügner, F. Spanier, and W. Winter, “Simplified models for photohadronic interactions in cosmic accelerators,” *Astrophys. J.* **721**, 630–652 (2010), arXiv:1002.1310 [astro-ph.HE].
- [84] M. G. Aartsen *et al.* (IceCube), “Measurement of South Pole ice transparency with the IceCube LED calibration system,” *Nucl. Instrum. Meth. A* **711**, 73–89 (2013), arXiv:1301.5361 [astro-ph.IM].
- [85] F. Feroz, M. P. Hobson, E. Cameron, and A. N. Pettitt, “Importance Nested Sampling and the MultiNest Algorithm,” (2013), arXiv:1306.2144 [astro-ph.IM].
- [86] Thomas P. Robitaille *et al.* (Astropy), “Astropy: A Community Python Package for Astronomy,” *Astron. Astrophys.* **558**, A33 (2013), arXiv:1307.6212 [astro-ph.IM].
- [87] J. Buchner *et al.*, “X-ray spectral modelling of the AGN obscuring region in the CDFS: Bayesian model selection and catalogue,” *Astron. Astrophys.* **564**, A125 (2014), arXiv:1402.0004 [astro-ph.HE].
- [88] Kfir Blum, Anson Hook, and Kohta Murase, “High energy neutrino telescopes as a probe of the neutrino mass mechanism,” (2014), arXiv:1408.3799 [hep-ph].
- [89] Mauricio Bustamante, John F. Beacom, and Kohta Murase, “Testing decay of astrophysical neutrinos with incomplete information,” *Phys. Rev. D* **95**, 063013 (2017), arXiv:1610.02096 [astro-ph.HE].
- [90] Aaron C. Vincent, Carlos A. Argelles, and Ali Kheirandish, “High-energy neutrino attenuation in the Earth and its associated uncertainties,” *JCAP* **1711**, 012 (2017), arXiv:1706.09895 [hep-ph].
- [91] IceCube Collaboration, *Search for contained neutrino events at energies greater than 1 TeV in 2 years of data* (2015 (accessed September 04, 2017)).
- [92] Spencer Klein, Private communication.
- [93] Yiqian Xu, “Measurement of High Energy NeutrinoNucleon Cross Section of Cascade Channel with IceCube,” Talk given at the International Cosmic Ray Conference 2017, July 15, 2017, Busan, <https://pos.sissa.it/301/978/>.
- [94] M. Honda, M. Sajjad Athar, T. Kajita, K. Kasahara, and S. Midorikawa, “Atmospheric neutrino flux calculation using the NRLMSISE-00 atmospheric model,” *Phys. Rev. D* **92**, 023004 (2015), arXiv:1502.03916 [astro-ph.HE].
- [95] E. V. Bugaev, Vadim A. Naumov, S. I. Sinegovsky, and E. S. Zaslavskaya, “Prompt Leptons in Cosmic Rays,” *Nuovo Cim. C* **12**, 41–73 (1989).
- [96] P. Gondolo, G. Ingelman, and M. Thunman, “Charm production and high-energy atmospheric muon and neutrino fluxes,” *Astropart. Phys.* **5**, 309–332 (1996), arXiv:hep-ph/9505417 [hep-ph].
- [97] L. Pasquali, M. H. Reno, and I. Sarcevic, “Lepton fluxes from atmospheric charm,” *Phys. Rev. D* **59**, 034020 (1999), arXiv:hep-ph/9806428 [hep-ph].
- [98] Rikard Enberg, Mary Hall Reno, and Ina Sarcevic, “Prompt neutrino fluxes from atmospheric charm,” *Phys. Rev. D* **78**, 043005 (2008), arXiv:0806.0418 [hep-ph].
- [99] Thomas K. Gaisser, “Atmospheric leptons,” *Proceedings, 17th International Symposium on Very High Energy Cosmic Ray Interactions (ISVHECRI 2012): Berlin, Germany, August 10-15, 2012*, EPJ Web Conf. **52**, 09004 (2013), arXiv:1303.1431 [hep-ph].
- [100] Atri Bhattacharya *et al.*, “Perturbative charm production and the prompt atmospheric neutrino flux in light of RHIC and LHC,” *JHEP* **06**, 110 (2015), arXiv:1502.01076 [hep-ph].
- [101] M. V. Garzelli, S. Moch, and G. Sigl, “Lepton fluxes from atmospheric charm revisited,” *JHEP* **10**, 115 (2015), arXiv:1507.01570 [hep-ph].
- [102] Rhorry Gauld, Juan Rojo, Luca Rottoli, Subir Sarkar, and Jim Talbert, “The prompt atmospheric neutrino flux in the light of LHCb,” *JHEP* **02**, 130 (2016), arXiv:1511.06346 [hep-ph].
- [103] Anatoli Fedynitch *et al.*, “ $MCEQ$  - numerical code for inclusive lepton flux calculations,” *Proceedings, 34th International Cosmic Ray Conference (ICRC 2015): The Hague, The Netherlands, July 30-August 6, 2015*, PoS **ICRC2015**, 1129 (2016).
- [104] Francis Halzen and Logan Wille, “Upper Limit on Forward Charm Contribution to Atmospheric Neutrino Flux,” (2016), arXiv:1601.03044 [hep-ph].
- [105] Francis Halzen and Logan Wille, “Charm contribution to the atmospheric neutrino flux,” *Phys. Rev. D* **94**, 014014 (2016), arXiv:1605.01409 [hep-ph].
- [106] Thomas K. Gaisser, “Atmospheric Neutrinos,” *Proceedings, 14th International Conference on Topics in Astroparticle and Underground Physics (TAUP 2015): Torino, Italy, September 7-11, 2015*, J. Phys. Conf. Ser. **718**, 052014 (2016), arXiv:1605.03073 [astro-ph.HE].
- [107] Atri Bhattacharya *et al.*, “Prompt atmospheric neutrino fluxes: perturbative QCD models and nuclear effects,” *JHEP* **11**, 167 (2016), arXiv:1607.00193 [hep-ph].
- [108] Ralph Engel *et al.*, “The hadronic interaction model Sibyll — past, present and future,” *Proceedings, 19th International Symposium on Very High Energy Cosmic Ray Interactions (ISVHECRI 2016): Moscow, Russia, August 22-27, 2016*, EPJ Web Conf. **145**, 08001 (2017).
- [109] Stefan Schonert, Thomas K. Gaisser, Elisa Resconi, and Olaf Schulz, “Vetoing atmospheric neutrinos in a high energy neutrino telescope,” *Phys. Rev. D* **79**, 043009 (2009), arXiv:0812.4308 [astro-ph].
- [110] Thomas K. Gaisser, Kyle Jero, Albrecht Karle, and Jakob van Santen, “Generalized self-veto probability for atmospheric neutrinos,” *Phys. Rev. D* **90**, 023009 (2014), arXiv:1405.0525 [astro-ph.HE].
- [111] Luis A. Anchordoqui *et al.*, “Cosmic Neutrino Pevatrons: A Brand New Pathway to Astronomy, Astrophysics, and Particle Physics,” *JHEAp* **1-2**, 1–30 (2014), arXiv:1312.6587 [astro-ph.HE].
- [112] M. G. Aartsen *et al.* (IceCube), “Neutrinos and Cosmic Rays Observed by IceCube,” *Adv. Space Research* (2017), 10.1016/j.asr.2017.05.030, arXiv:1701.03731 [astro-ph.HE].



- [113] Tamar Kashti and Eli Waxman, “Flavoring astrophysical neutrinos: Flavor ratios depend on energy,” *Phys. Rev. Lett.* **95**, 181101 (2005), arXiv:astro-ph/0507599.
- [114] Paolo Lipari, Maurizio Lusignoli, and Davide Meloni, “Flavor Composition and Energy Spectrum of Astrophysical Neutrinos,” *Phys. Rev. D* **75**, 123005 (2007), arXiv:0704.0718 [astro-ph].
- [115] Olga Mena, Sergio Palomares-Ruiz, and Aaron C. Vincent, “On the flavor composition of the high-energy neutrino events in IceCube,” *Phys. Rev. Lett.* **113**, 091103 (2014), arXiv:1404.0017 [astro-ph.HE].
- [116] Mauricio Bustamante, John F. Beacom, and Walter Winter, “Theoretically palatable flavor combinations of astrophysical neutrinos,” *Phys. Rev. Lett.* **115**, 161302 (2015), arXiv:1506.02645 [astro-ph.HE].
- [117] Aaron C. Vincent, Sergio Palomares-Ruiz, and Olga Mena, “Analysis of the 4-year IceCube high-energy starting events,” *Phys. Rev. D* **94**, 023009 (2016), arXiv:1605.01556 [astro-ph.HE].
- [118] M. G. Aartsen *et al.* (IceCube), “Flavor Ratio of Astrophysical Neutrinos above 35 TeV in IceCube,” *Phys. Rev. Lett.* **114**, 171102 (2015), arXiv:1502.03376 [astro-ph.HE].
- [119] Kohta Murase, Markus Ahlers, and Brian C. Lacki, “Testing the Hadronuclear Origin of PeV Neutrinos Observed with IceCube,” *Phys. Rev. D* **88**, 121301 (2013), arXiv:1306.3417 [astro-ph.HE].
- [120] Kohta Murase, Dafne Guetta, and Markus Ahlers, “Hidden Cosmic-Ray Accelerators as an Origin of TeV-PeV Cosmic Neutrinos,” *Phys. Rev. Lett.* **116**, 071101 (2016), arXiv:1509.00805 [astro-ph.HE].
- [121] S. R. Kelner, Felix A. Aharonian, and V. V. Bugayov, “Energy spectra of gamma-rays, electrons and neutrinos produced at proton-proton interactions in the very high energy regime,” *Phys. Rev. D* **74**, 034018 (2006), [Erratum: *Phys. Rev. D* 79, 039901 (2009)], arXiv:astro-ph/0606058 [astro-ph].
- [122] Georges Aad *et al.* (ATLAS), “Search for strong gravity signatures in same-sign dimuon final states using the ATLAS detector at the LHC,” *Phys. Lett. B* **709**, 322–340 (2012), arXiv:1111.0080 [hep-ex].
- [123] Serguei Chatrchyan *et al.* (CMS), “Search for microscopic black holes in  $pp$  collisions at  $\sqrt{s} = 7$  TeV,” *JHEP* **04**, 061 (2012), arXiv:1202.6396 [hep-ex].
- [124] Marek Paul Kowalski, *Search for neutrino induced cascades with the AMANDA-II detector*, Ph.D. thesis, Humboldt U., Berlin (2004).
- [125] Shirley Weishi Li, Mauricio Bustamante, and John F. Beacom, “Echo Technique to Distinguish Flavors of Astrophysical Neutrinos,” (2016), arXiv:1606.06290 [astro-ph.HE].
- [126] M. G. Aartsen *et al.* (IceCube), “Searches for Extended and Point-like Neutrino Sources with Four Years of IceCube Data,” *Astrophys. J.* **796**, 109 (2014), arXiv:1406.6757 [astro-ph.HE].
- [127] M. G. Aartsen *et al.* (IceCube), “Constraints on Galactic Neutrino Emission with Seven Years of IceCube Data,” *Astrophys. J.* **849**, 67 (2017), arXiv:1707.03416 [astro-ph.HE].
- [128] Andrii Neronov and Dmitry V. Semikoz, “Evidence the Galactic contribution to the IceCube astrophysical neutrino flux,” *Astropart. Phys.* **75**, 60–63 (2016), arXiv:1509.03522 [astro-ph.HE].
- [129] Peter B. Denton, Danny Marfatia, and Thomas J. Weiler, “The Galactic Contribution to IceCube’s Astrophysical Neutrino Flux,” *JCAP* **1708**, 033 (2017), arXiv:1703.09721 [astro-ph.HE].
- [130] M. G. Aartsen *et al.* (IceCube), “IceCube-Gen2: A Vision for the Future of Neutrino Astronomy in Antarctica,” (2014), arXiv:1412.5106 [astro-ph.HE].
- [131] S. Adrian-Martinez *et al.* (KM3Net), “Letter of intent for KM3NeT 2.0,” *J. Phys. G* **43**, 084001 (2016), arXiv:1601.07459 [astro-ph.IM].
- [132] M. G. Aartsen *et al.* (IceCube), “Measurements using the inelasticity distribution of multi-TeV neutrino interactions in IceCube,” (2018), arXiv:1808.07629 [hep-ex].
- [133] Luis A. Anchordoqui, Carlos A. Garcia Canal, Haim Goldberg, Daniel Gomez Dumm, and Francis Halzen, “Probing leptoquark production at IceCube,” *Phys. Rev. D* **74**, 125021 (2006), arXiv:hep-ph/0609214 [hep-ph].
- [134] Mathieu Ribordy and Alexei Yu Smirnov, “Improving the neutrino mass hierarchy identification with inelasticity measurement in PINGU and ORCA,” *Phys. Rev. D* **87**, 113007 (2013), arXiv:1303.0758 [hep-ph].
- [135] L. N. Lipatov, “Reggeization of the Vector Meson and the Vacuum Singularity in Nonabelian Gauge Theories,” *Sov. J. Nucl. Phys.* **23**, 338–345 (1976), [*Yad. Fiz.* 23, 642 (1976)].
- [136] E. A. Kuraev, L. N. Lipatov, and Victor S. Fadin, “Multi - Reggeon Processes in the Yang-Mills Theory,” *Sov. Phys. JETP* **44**, 443–450 (1976), [*Zh. Eksp. Teor. Fiz.* 71, 840 (1976)].
- [137] E. A. Kuraev, L. N. Lipatov, and Victor S. Fadin, “The Pomeranchuk Singularity in Nonabelian Gauge Theories,” *Sov. Phys. JETP* **45**, 199–204 (1977), [*Zh. Eksp. Teor. Fiz.* 72, 377 (1977)].
- [138] I. I. Balitsky and L. N. Lipatov, “The Pomeranchuk Singularity in Quantum Chromodynamics,” *Sov. J. Nucl. Phys.* **28**, 822–829 (1978), [*Yad. Fiz.* 28, 1597 (1978)].
- [139] Francois Gelis, Edmond Iancu, Jamal Jalilian-Marian, and Raju Venugopalan, “The Color Glass Condensate,” *Ann. Rev. Nucl. Part. Sci.* **60**, 463–489 (2010), arXiv:1002.0333 [hep-ph].
- [140] Ernest M. Henley and Jamal Jalilian-Marian, “Ultra-high energy neutrino-nucleon scattering and parton distributions at small  $x$ ,” *Phys. Rev. D* **73**, 094004 (2006), arXiv:hep-ph/0512220 [hep-ph].
- [141] Luis A. Anchordoqui, Amanda M. Cooper-Sarkar, Dan Hooper, and Subir Sarkar, “Probing low- $x$  QCD with cosmic neutrinos at the Pierre Auger Observatory,” *Phys. Rev. D* **74**, 043008 (2006), arXiv:hep-ph/0605086 [hep-ph].
- [142] Valerio Bertone, Rhorry Gauld, and Juan Rojo, “Neutrino Telescopes as QCD Microscopes,” (2018), arXiv:1808.02034 [hep-ph].
- [143] P. Allison *et al.*, “Design and Initial Performance of the Askaryan Radio Array Prototype EeV Neutrino Detector at the South Pole,” *Astropart. Phys.* **35**, 457–477 (2012), arXiv:1105.2854 [astro-ph.IM].
- [144] P. Allison *et al.* (ARA), “First Constraints on the Ultra-High Energy Neutrino Flux from a Prototype Station of the Askaryan Radio Array,” *Astropart. Phys.* **70**, 62–80 (2015), arXiv:1404.5285 [astro-ph.HE].
- [145] P. Allison *et al.* (ARA), “Performance of two Askaryan Radio Array stations and first results in the search for ultrahigh energy neutrinos,” *Phys. Rev. D* **93**, 082003

- (2016), arXiv:1507.08991 [astro-ph.HE].
- [146] Steven W. Barwick, “ARIANNA: A New Concept for UHE Neutrino Detection,” *TeV Particle Astrophysics. Proceedings, 2nd Workshop, Madison, USA, August 28-31, 2006*, J. Phys. Conf. Ser. **60**, 276–283 (2007), arXiv:astro-ph/0610631 [astro-ph].
- [147] S. W. Barwick *et al.* (ARIANNA), “A First Search for Cosmogenic Neutrinos with the ARIANNA Hexagonal Radio Array,” *Astropart. Phys.* **70**, 12–26 (2015), arXiv:1410.7352 [astro-ph.HE].
- [148] Jaime Alvarez-Muiz *et al.* (GRAND), “The Giant Radio Array for Neutrino Detection (GRAND): Science and Design,” (2018), arXiv:1810.09994 [astro-ph.HE].
- [149] Angela V. Olinto *et al.*, “POEMMA: Probe Of Extreme Multi-Messenger Astrophysics,” *Proceedings, 35th International Cosmic Ray Conference (ICRC 2017): Bexco, Busan, Korea, July 12-20, 2017*, PoS **ICRC2017**, 542 (2017), arXiv:1708.07599 [astro-ph.IM].
- [150] L. A. Anchordoqui *et al.*, “Upper bounds on the neutrino-nucleon inelastic cross section,” *JCAP* **0506**, 013 (2005), arXiv:hep-ph/0410136 [hep-ph].

## Appendix A: Shower rates in IceCube

Below,  $\nu$  stands for both neutrino and anti-neutrino, unless otherwise specified.

### 1. Neutrino-induced events

High-energy neutrinos deep-inelastic-scatter off nucleons in the Antarctic ice. Charged-current (CC) interactions make charged leptons:  $\nu_l + N \rightarrow l + X$  ( $l = e, \mu, \tau$ ), where  $N$  is either a neutron or a proton, and  $X$  are final-state hadrons, mostly pions. Neutral-current (NC) interactions make neutrinos:  $\nu_l + N \rightarrow \nu_l + X$ . Outgoing hadrons receive a fraction  $y$  of the initial neutrino energy — known as the inelasticity — while outgoing leptons receive  $(1 - y)$  of it. Outgoing charged particles make Cherenkov light that is collected by IceCube photomultipliers buried in the ice.

The muon from a  $\nu_\mu$  CC interaction leaves a track of Cherenkov light several kilometers long that, if it crosses the instrumented volume of IceCube, is typically clearly identifiable. Muon tracks also come from the decay of taus, made by  $\nu_\tau$  CC interactions, into muons, which occurs 17% of the time.

All other final-state charged particles create particle showers localized around the interaction vertex. A shower from final-state hadrons has a high neutron and pion content — a hadronic shower. In a NC interaction, this is the only shower, since the final-state neutrino exits the detector. In a  $\nu_e$  CC interaction, the electron creates an additional shower that consists mainly of electrons, positrons, and photons, and has low hadronic content — an electromagnetic shower. In a  $\nu_\tau$  CC interaction, the tau decay creates a hadronic shower 66% of the time and an electromagnetic shower 17% of the time (the remaining 17% of the time, the tau decays to a muon, which creates track). IceCube does not resolve individually the lepton- and hadron-initiated showers; they are detected as a superposition. Also, it is unable to distinguish between neutrinos and anti-neutrinos based only on total energy deposition.

Shower detection in IceCube is calorimetric: if the shower starts well within the detector — like in HESE showers — all of the shower energy is deposited in the ice, and most of it is collected by the photomultipliers. The relation between the energy of the shower  $E_{\text{sh}}$  and the energy of the incoming neutrino  $E_\nu$  depends on the flavor of the neutrino and the type of the interaction. In a  $\nu_e$  CC interaction, all of the neutrino energy is given to the electromagnetic and hadronic showers. In a  $\nu_\tau$  CC interaction, about 30% of the tau energy is lost to neutrinos at decay, after averaging over all decay channels. In a NC interaction, on average, the shower energy is only  $\langle y \rangle E_\nu$ , where  $\langle y \rangle$  is the average inelasticity. Around  $E_\nu = 1$  PeV,  $\langle y \rangle \approx 0.25$  for neutrinos and anti-neutrinos, and for CC and NC interactions [55]. In summary, the average fraction  $f_{l,t}$  of neutrino energy carried by the shower in a  $\nu_l$  or  $\bar{\nu}_l$  interaction of type  $t$  (CC or NC) is [89]

$$f_{l,t} \equiv \frac{E_{\text{sh}}}{E_\nu} \simeq \begin{cases} 1 & \text{for } l = e \text{ and } t = \text{CC} \\ [\langle y \rangle + 0.7(1 - \langle y \rangle)] \simeq 0.8 & \text{for } l = \tau \text{ and } t = \text{CC} \\ \langle y \rangle \simeq 0.25 & \text{for } l = e, \mu, \tau \text{ and } t = \text{NC} \end{cases} . \quad (\text{A1})$$

(See also Ref. [88], where different decay modes of the tau are treated separately.) Since  $f_{l,\text{NC}}$  is small, and since the atmospheric and astrophysical neutrino fluxes fall steeply with energy ( $\propto E_\nu^{-\gamma}$ ), the NC contribution to the total shower rate is sub-dominant.

## 2. Energy and angular spectrum of showers

In the main text, we established that sensitivity to the neutrino-nucleon cross section comes from the attenuation of the neutrino flux as it propagates inside the Earth, which depends on neutrino energy and direction. Therefore, to constrain the cross section, we need to compute the doubly differential spectrum — in energy and arrival direction — of showers in IceCube. To do that, we extend the “theorist’s approach” from Refs. [76, 89] (see also Ref. [88]) to account for the angular distribution:

$$\frac{d^2 N_{\text{sh}}}{dE_{\text{sh}} d \cos \theta_z} = \frac{d^2 N_{\text{sh},e}^{\text{CC}}}{dE_{\text{sh}} d \cos \theta_z} + \text{Br}_{\tau \rightarrow \text{sh}} \frac{d^2 N_{\text{sh},\tau}^{\text{CC}}}{dE_{\text{sh}} d \cos \theta_z} + \sum_{l=e,\mu,\tau} \frac{d^2 N_{\text{sh},l}^{\text{NC}}}{dE_{\text{sh}} d \cos \theta_z}, \quad (\text{A2})$$

where  $\theta_z$  is the zenith angle of the incoming neutrino (the normal to the South Pole is at  $\theta_z = 0$ ),  $\text{Br}_{\tau \rightarrow \text{sh}} = 0.83$  is the branching ratio of tau decays that make a shower, and

$$\frac{d^2 N_{\text{sh},l}^{\text{CC}}}{dE_{\text{sh}} d \cos \theta_z}(E_{\text{sh}}, \cos \theta_z) \simeq -2\pi \rho_{\text{ice}} N_A V T \left\{ \Phi_l(E_\nu) \sigma_{\nu N}^{\text{CC}}(E_\nu) e^{-\tau_{\nu N}(E_\nu, \theta_z)} + \Phi_{\bar{l}}(E_\nu) \sigma_{\bar{\nu} N}^{\text{CC}}(E_\nu) e^{-\tau_{\bar{\nu} N}(E_\nu, \theta_z)} \right\} \Big|_{E_\nu = E_{\text{sh}}/f_{l,\text{CC}}}, \quad (\text{A3})$$

for showers initiated by CC interactions of a flux of  $\nu_l$  ( $\Phi_l$ ) and  $\bar{\nu}_l$  ( $\Phi_{\bar{l}}$ ). On the right-hand side of Eq. (A3), the neutrino energy is computed from the shower energy by means of Eq. (A1). The number of nucleon targets inside the instrumented volume is  $\rho_{\text{ice}} N_A V$ , with  $\rho_{\text{ice}} \approx 0.92 \text{ g cm}^{-3}$  the density of ice,  $N_A$  the Avogadro number, and  $V \approx 1 \text{ km}^3$  the volume of IceCube. The expression for showers from NC interactions,  $d^2 N_{\text{sh},l}^{\text{NC}}/dE_{\text{sh}}/d \cos \theta_z$ , is obtained from Eq. (A3) by changing  $\sigma_{\nu N}^{\text{CC}} \rightarrow \sigma_{\nu N}^{\text{NC}}$ ,  $\sigma_{\bar{\nu} N}^{\text{CC}} \rightarrow \sigma_{\bar{\nu} N}^{\text{NC}}$ , and  $f_{l,\text{CC}} \rightarrow f_{l,\text{NC}}$ .

To calculate the attenuation factors  $e^{-\tau_{\nu N}}$  and  $e^{-\tau_{\bar{\nu} N}}$ , consider an incoming flux of neutrinos with energy  $E_\nu$  and zenith angle  $\theta_z$ . Inside the Earth, which has approximate radius  $R_\oplus = 6371 \text{ km}$ , the neutrinos travel a distance

$$D(\theta_z) = \sqrt{(R_\oplus^2 - 2R_\oplus d) \cos^2 \theta_z + 2R_\oplus d} - (R_\oplus - d) \cos \theta_z \quad (\text{A4})$$

before reaching IceCube, which is buried at a depth  $d = 1.5 \text{ km}$ . We compute the average Earth density  $\langle \rho_\oplus(\theta_z) \rangle = (1/D(\theta_z)) \int_0^{D(\theta_z)} \rho_\oplus(x) dx$  encountered by the neutrino using the density profile  $\rho_\oplus$  from the Preliminary Reference Earth Model (PREM) [55, 79]. (Variations between PREM and other Earth density models are at the level of 5%, so they can be neglected given the size of the errors in our extracted cross sections.) To a good approximation, Earth matter is isoscalar — composed of equal numbers of neutrons and protons — so the average nucleon mass is  $m_N = (m_p + m_n)/2$ . Thus, the  $\nu N$  interaction length (for any flavor) is

$$L_{\nu N}(E_\nu, \theta_z) = \frac{m_N}{\langle \rho_\oplus(\theta_z) \rangle} \left( \frac{1}{\sigma_{\nu N}^{\text{CC}}(E_\nu) + \sigma_{\nu N}^{\text{NC}}(E_\nu)} \right), \quad (\text{A5})$$

and, from this, the attenuation factor is

$$e^{-\tau_{\nu N}(E_\nu, \theta_z)} \equiv e^{-D(\theta_z)/L_{\nu N}(E_\nu, \theta_z)}. \quad (\text{A6})$$

For anti-neutrinos, the interaction length and attenuation factor have identical expressions, with  $\nu \rightarrow \bar{\nu}$ .

Figure A1 shows the interaction length as a function of zenith angle, computed, for illustration, using the standard prediction of the high-energy cross section from Ref. [59]. There, we have separated the NC and CC interactions lengths, to illustrate the fact that the CC cross section is predicted to be  $\sim 3$  times higher than the NC cross section.

Figure A2 shows the corresponding attenuation factors. Close to the horizon, attenuation is small ( $e^{-\tau_{\nu N}} \approx 1$ ), except at very high energies, while above the horizon, attenuation is negligible at all energies. Kinks on the curves reflect transitions between layers of different density inside the Earth [79].

The authors of Refs. [78, 90] performed a more comprehensive calculation of attenuation, treating different flavors of neutrinos and anti-neutrinos separately. Our results are compatible with theirs, except for the inclusion of charged-current regenerations of  $\nu_\tau$  and neutral-current regeneration of all flavors, which we have ignored since they affect the flux arriving at the detector only at the  $\sim 10\%$  level, which is unresolvable in the face of the large cross-section uncertainties we find.

The contribution of atmospheric neutrinos to the HESE event rate is reduced by using the outer layer of PMTs as a veto. When a contained event occurs, if the outer PMTs detect the passage of a muon that was made in the same atmospheric interaction as the neutrino responsible for the contained event, then the event is tagged as

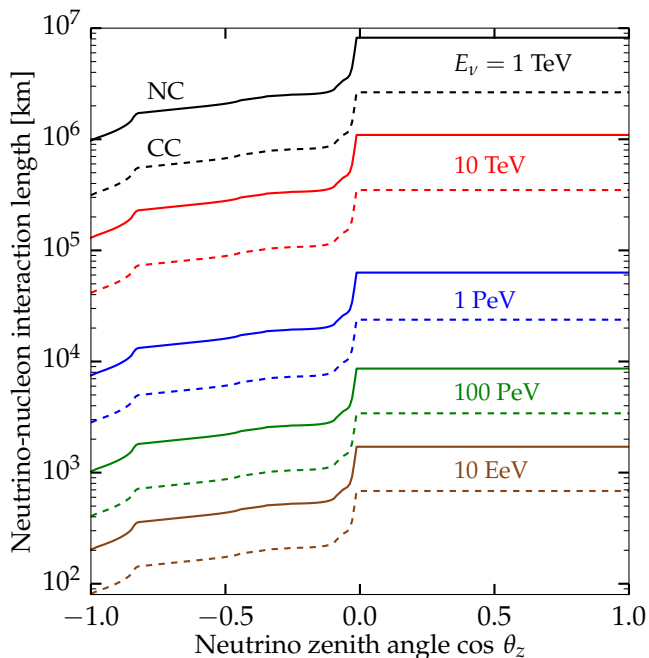


FIG. A1. Neutrino-nucleon interaction length for neutrinos inside the Earth, as a function of zenith angle, for different neutrino energies. We have separately calculated the length for neutral-current (NC, solid lines) and charged-current (CC, dashed lines) interactions. The  $\nu N$  cross sections are taken from Ref. [59]. Interaction lengths for anti-neutrinos (not shown) are about 60% higher, due to the smaller cross section.

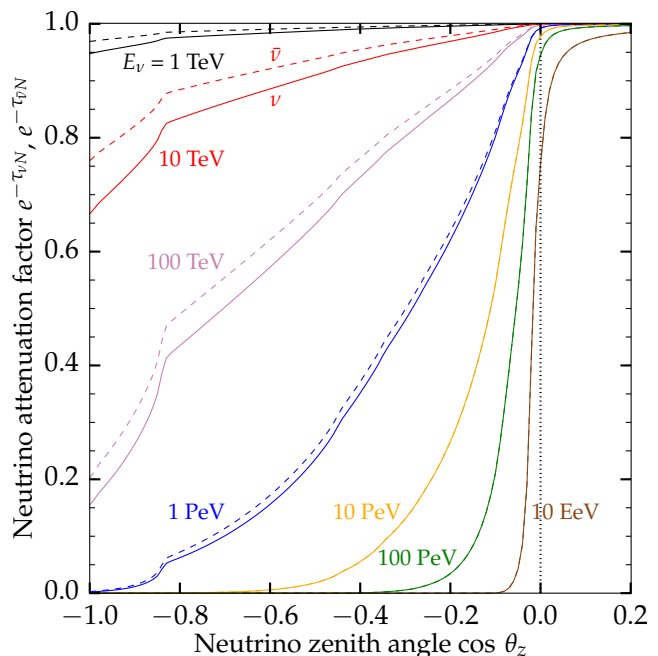


FIG. A2. In-Earth attenuation factors for neutrinos (solid lines) and anti-neutrinos (dashed lines), as a function of zenith angle, calculated for different neutrino energies and using the central values of the  $\nu N$  cross sections from Ref. [59].

background. Since the atmospheric neutrino flux falls faster with energy than the astrophysical flux, the probability that an atmospheric neutrino passes the veto falls with energy. We have calculated the passing probability following Refs. [109, 110], and multiplied Eq. (A3) by it when calculating the rate of showers due to atmospheric neutrinos.

In our analysis, we have not considered the fact that  $\sim 30\%$  of IceCube contained tracks are mis-identified as showers [118], either because they deposit too little energy or because they occur too close to the edges of the detector. In these events, because the shower is due mainly to the final-state hadrons, the deposited energy is small, *i.e.*,  $E_{\text{dep}} \approx yE_\nu$ . Hence, like NC showers, the contribution of mis-reconstructed muon tracks is sub-dominant. Therefore, they should not significantly affect our ability to present the extracted cross sections as functions of  $E_\nu \approx E_{\text{dep}}$ .

At energies above 2 PeV — beyond those available in the 6-year HESE sample — we would need also to take into account showers created by  $\bar{\nu}_e$  triggering the Glashow resonance [66] on electrons ( $\bar{\nu}_e + e \rightarrow W$ ), and the subsequent shower produced by the decay of the on-shell  $W$ . At these energies, the shower rate due to neutrino-nucleon interactions is negligible, so any detection can be attributed to the Glashow resonance. Thus, its eventual detection would single out the  $\bar{\nu}_e$  flux and help break the degeneracy between neutrino and anti-neutrino cross sections.

### 3. Astrophysical and atmospheric neutrino spectra

For astrophysical neutrinos, we choose a power-law spectrum, in agreement with IceCube findings. We assume equal proportions of each flavor in the flux, *i.e.*, the flavor ratios are  $(f_{e,\oplus} : f_{\mu,\oplus} : f_{\tau,\oplus}) = (\frac{1}{3} : \frac{1}{3} : \frac{1}{3})$ , which is compatible with IceCube results [36, 118] and with theoretical predictions of standard flavor mixing [68, 78, 113–117]. We also assume equal proportion of neutrinos and anti-neutrinos in the flux, which is expected from neutrino production in proton-proton interactions [121] and, at high energies, in proton-photon interactions [81, 83]. The spectrum of  $\nu_l$  is

$$\Phi_l^{\text{ast}}(E_\nu) = \Phi_{\nu,0} \left( \frac{E_\nu}{100 \text{ TeV}} \right)^{-\gamma}, \quad (\text{A7})$$

where  $\Phi_{\nu,0}$  is the normalization per flavor of neutrino or anti-neutrino (in units of  $\text{GeV}^{-1} \text{ cm}^{-2} \text{ s}^{-1} \text{ sr}^{-1}$ ) and  $\gamma$  is the spectral index, common to all flavors, and to neutrinos and anti-neutrinos. Equation (A7) also describes the spectrum

of  $\bar{\nu}_l$ . Our analysis (Appendix B) finds values of  $\Phi_{\nu,0}$  (implicitly) and  $\gamma$  inside each energy via a fit to IceCube data.

For conventional atmospheric neutrinos, created in the decays of pions and kaons, we use the recent calculation of  $\nu_e$ ,  $\bar{\nu}_e$ ,  $\nu_\mu$ , and  $\bar{\nu}_\mu$  fluxes by Honda *et al.* from Ref. [94].

We do not include prompt atmospheric neutrinos [95–101, 103–108] in our analysis because recent searches have repeatedly failed to find them [26, 31–38]. However, in a full analysis of cross sections performed by the IceCube Collaboration, using more HESE data, the normalization of the prompt neutrino flux could be left as an additional free parameter to be determined by a fit, like it was done in Ref. [7].

In our calculations, we convert declination and right ascension to zenith angle using the `astropy` package [86]. Since the Earth density profile model that we use is spherically symmetric [55, 79], the single zenith angle coordinate is sufficient to calculate the neutrino attenuation inside the Earth.

#### 4. Energy and angular resolution of the detector

To compare our predicted shower spectra with the spectrum of observed HESE showers, we need to account for the energy resolution and angular resolution of the detector. We do that by convolving the true spectrum, Eq. (A2), with two functions that parametrize the detector resolution, *i.e.*,

$$\frac{d^2 N_{\text{sh}}}{dE_{\text{dep}} d \cos \theta_z} = \int dE_{\text{sh}} \int d \cos \theta'_z \frac{d^2 N_{\text{sh}}}{dE_{\text{sh}} d \cos \theta'_z} R_E(E_{\text{sh}}, E_{\text{dep}}, \sigma_E(E_{\text{sh}})) R_\theta(\cos \theta'_z, \cos \theta_z, \sigma_{\cos \theta_z}), \quad (\text{A8})$$

where the energy resolution function  $R_E$  and the angular resolution function  $R_\theta$  are Gaussians centered around the true values  $E_{\text{sh}}$  and  $\cos \theta'_z$ , respectively.

For the energy resolution function, we adopt [78, 89, 117]

$$R_E(E_{\text{sh}}, E_{\text{dep}}, \sigma_E(E_{\text{sh}})) = \frac{1}{\sqrt{2\pi\sigma_E^2(E_{\text{sh}})}} \exp\left[-\frac{(E_{\text{sh}} - E_{\text{dep}})^2}{2\sigma_E^2(E_{\text{sh}})}\right], \quad (\text{A9})$$

with  $\sigma_E(E_{\text{sh}}) = 0.1E_{\text{sh}}$ , consistent with the value reported by IceCube [77].

For the angular resolution function of showers, there is no conventional parametrization, to the best of our knowledge. We adopt a resolution function in cosine of the zenith angle, *i.e.*,

$$R_\theta(\cos \theta'_z, \cos \theta_z, \sigma_{\cos \theta_z}) = \frac{1}{\sqrt{2\pi\sigma_{\cos \theta_z}^2}} \exp\left[-\frac{(\cos \theta'_z - \cos \theta_z)^2}{2\sigma_{\cos \theta_z}^2}\right]. \quad (\text{A10})$$

The dispersion  $\sigma_{\cos \theta_z}$  is calculated, for a given value of  $\theta_z = \arccos(\cos \theta_z)$ , as the average between the upward and downward fluctuation in the cosine, *i.e.*,

$$\sigma_{\cos \theta_z} \equiv \frac{1}{2} [|\cos(\theta_z + \sigma_{\theta_z}) - \cos \theta_z| + |\cos(\theta_z - \sigma_{\theta_z}) - \cos \theta_z|], \quad (\text{A11})$$

where we choose a representative value of  $\sigma_{\theta_z} = 15^\circ$  for the dispersion of the angle itself. In reality,  $\sigma_{\theta_z}$  is a function of deposited shower energy, with the resolution deteriorating towards low energies, as illustrated in Fig. 14 of Ref. [77]. Our simplified choice captures the mean angular resolution of HESE showers without attempting to extract a proper resolution function from the aforementioned figure.

#### 5. Lower-energy IceCube contained events

We avoid using lower-energy contained events — Medium Energy Starting Events (MESE) [34, 91], down to  $E_{\text{dep}} \approx 1$  TeV — due to the difficulty of correctly modeling how light absorption and scattering by ice distort the angular acceptance of IceCube [84, 92]. For HESE, these effects are mitigated due to their higher light yield (see, *e.g.*, Fig. 3 in Ref. [93]), so we ignore them here without introducing large errors.

#### Appendix B: Statistical analysis

To extract the neutrino-nucleon cross section, we compare our test shower spectra (see Appendix A) with the observed spectrum of IceCube HESE [26–29] showers. We bin showers in  $E_{\text{dep}}$  — which, for showers, approximates

TABLE II. Best-fit values and  $1\sigma$  uncertainties of the nuisance parameters in each energy bin: number of showers due to atmospheric neutrinos  $N_{\text{sh}}^{\text{atm}}$ , number of showers due to astrophysical neutrinos  $N_{\text{sh}}^{\text{ast}}$ , and astrophysical spectral index  $\gamma$ .

$E_\nu$ [TeV]	$N_{\text{sh}}^{\text{atm}}$	$N_{\text{sh}}^{\text{ast}}$	$\gamma$
18–50	$4.2 \pm 4.9$	$11.4 \pm 3.5$	$2.38 \pm 0.31$
50–100	$6.3 \pm 5.3$	$11.7 \pm 4.5$	$2.43 \pm 0.31$
100–400	$6.4 \pm 6.0$	$12.9 \pm 5.2$	$2.49 \pm 0.31$
400–2004	$1.2 \pm 1.0$	$1.73 \pm 0.89$	$2.37 \pm 0.32$

$E_\nu$  (since NC showers are sub-dominant; see Appendix A). Because of limited data, we use only four bins: 18–50 TeV, 50–100 TeV, 100–400 TeV, and 400–2004 TeV. The first three bins contain roughly the same number of events each (17–20), while the final bin contains only 3 events; Table I contains the event numbers. We perform a fit to shower data in each bin independently, as described below, employing a maximum likelihood method modeled after Refs. [78, 117].

In a bin containing  $N_{\text{sh}}^{\text{obs}}$  observed showers, the likelihood is

$$\mathcal{L} = \frac{e^{-(N_{\text{sh}}^{\text{atm}} + N_{\text{sh}}^{\text{ast}})} N_{\text{sh}}^{\text{obs}}}{N_{\text{sh}}^{\text{obs}}!} \prod_{i=1}^{N_{\text{sh}}^{\text{obs}}} \mathcal{L}_i, \quad (\text{B1})$$

where  $N_{\text{sh}}^{\text{atm}}$  is the number of showers due to atmospheric neutrinos and  $N_{\text{sh}}^{\text{ast}}$  is the number of showers due to astrophysical neutrinos. The partial likelihood  $\mathcal{L}_i$  of the  $i$ -th shower in this bin captures the relative probability of the shower being from an atmospheric or an astrophysical neutrino. It is computed as

$$\mathcal{L}_i = N_{\text{sh}}^{\text{atm}} \mathcal{P}_i^{\text{atm}} + N_{\text{sh}}^{\text{ast}} \mathcal{P}_i^{\text{ast}}, \quad (\text{B2})$$

where  $\mathcal{P}_i^{\text{atm}}$  and  $\mathcal{P}_i^{\text{ast}}$  are, respectively, the probability distribution for this shower to be generated by the atmospheric neutrino flux and by the astrophysical neutrino flux. These are calculated as

$$\mathcal{P}_i^{\text{atm}} = \left( \int_{E_{\text{dep}}^{\text{min}}}^{E_{\text{dep}}^{\text{max}}} dE_{\text{dep}} \int_{-1}^1 d \cos \theta_z \frac{d^2 N_{\text{sh}}^{\text{atm}}}{dE_{\text{dep}} d \cos \theta_z} \right)^{-1} \left( \frac{d^2 N_{\text{sh}}^{\text{atm}}}{dE_{\text{dep}} d \cos \theta_z} \Big|_{E_{\text{dep},i}, \cos \theta_{z,i}} \right), \quad (\text{B3})$$

$$\mathcal{P}_i^{\text{ast}} = \left( \int_{E_{\text{dep}}^{\text{min}}}^{E_{\text{dep}}^{\text{max}}} dE_{\text{dep}} \int_{-1}^1 d \cos \theta_z \frac{d^2 N_{\text{sh}}^{\text{ast}}}{dE_{\text{dep}} d \cos \theta_z} \right)^{-1} \left( \frac{d^2 N_{\text{sh}}^{\text{ast}}}{dE_{\text{dep}} d \cos \theta_z} \Big|_{E_{\text{dep},i}, \cos \theta_{z,i}} \right), \quad (\text{B4})$$

where  $E_{\text{dep}}^{\text{min}}$  and  $E_{\text{dep}}^{\text{max}}$  are the boundaries of the energy bin. The double integrals represent the number of events in the energy bin, summed over all arrival directions. The shower spectra  $d^2 N_{\text{sh}}/dE_{\text{dep}}/d \cos \theta_z$  for atmospheric and astrophysical neutrinos are computed in Appendix A. Equations (B3) and (B4) depend on the four cross sections  $\sigma_{\nu N}^{\text{CC}}$ ,  $\sigma_{\bar{\nu} N}^{\text{CC}}$ ,  $\sigma_{\nu N}^{\text{NC}}$ , and  $\sigma_{\bar{\nu} N}^{\text{NC}}$ . We assume the cross sections to be constant within each bin. Equation (B4) depends also on the astrophysical spectral index  $\gamma$ .

The full likelihood for one energy bin, Eq. (B1), is a function of 7 free parameters:  $N_{\text{sh}}^{\text{atm}}$ ,  $N_{\text{sh}}^{\text{ast}}$ ,  $\sigma_{\nu N}^{\text{CC}}$ ,  $\sigma_{\bar{\nu} N}^{\text{CC}}$ ,  $\sigma_{\nu N}^{\text{NC}}$ ,  $\sigma_{\bar{\nu} N}^{\text{NC}}$ , and  $\gamma$ . However, the three simplifying assumptions introduced in the main text reduce the number of free parameters to 4:  $\sigma_{\nu N}^{\text{CC}}$ ,  $N_{\text{sh}}^{\text{atm}}$ ,  $N_{\text{sh}}^{\text{ast}}$ ,  $\gamma$ . The latter three are treated as nuisance parameters.

In each energy bin, we independently vary and fit for the four free parameters. We choose a flat prior for all of the parameters. To find the maximum of the likelihood, we use `MultiNest`, an efficient implementation of the multinodal nested sampling algorithm [80, 82, 85], via the Python module `PyMultiNest` [87]. The fitting procedure returns, in each bin, the best-fit value and uncertainty of  $\sigma_{\nu N}^{\text{CC}}$ . From this, we calculate  $\sigma_{\bar{\nu} N}^{\text{CC}} = \langle \sigma_{\bar{\nu} N}^{\text{CC}} / \sigma_{\nu N}^{\text{CC}} \rangle \cdot \sigma_{\nu N}^{\text{CC}}$ ; the values of  $\langle \sigma_{\bar{\nu} N}^{\text{CC}} / \sigma_{\nu N}^{\text{CC}} \rangle$  are in Table I. Because, in our analysis, the  $\nu N$  and  $\bar{\nu} N$  cross sections are not independent, we present the average between them,  $(\sigma_{\nu N}^{\text{CC}} + \sigma_{\bar{\nu} N}^{\text{CC}})/2$ . Table I, in the main text, shows the results, marginalized over the nuisance parameters.

Table II shows, for completeness, the resulting values of the nuisance parameters after fitting. In the main text, they are used to isolate the statistical and systematic uncertainties.